A note on a traveling wave on an extensible capsule membrane –with bending rigidity– in poiseuille flow

M.A.H. Reyes and F. Méndez-Lavielle
Facultad de Ingeniería, Universidad Nacional Autónoma de México,
e-mail: mreyes@maxwell.iimatercu.unam.mx

E. Geffroy
Instituto de Investigaciones en Materiales, Universidad Nacional Autónoma de México.

Recibido el 29 de enero de 2010; aceptado el 3 de marzo de 2010

We consider the effects of the bending rigidity of a capsule membrane convected by Poiseuille flow. We show numerically how the transition from a "discoidal shape" to "V shape or cordial form" capsules is mediated by travelling waves responsible for the required change in curvature. We show numerically that the wave velocity is an increasing function of both the rigidity of the membrane and the pressure gradient. A qualitative explanation of the observation is given in terms of a Burger's type equation for the curvature.

Keywords: Capsules; waves; Poiseuille flow.

Consideramos los efectos de la rigidez de doblez de una capsula convectada por el flujo de Poiseville. Demostramos numéricamente cómo la transición de una "forma discoide" a una tipo "V o cordial" de las cápsulas son mediante ondas viajeras responsables del cambio requerido en curvatura. Demostramos numéricamente que la velocidad de onda es una función de aumento de la rigidez de la membrana y del gradiente de presión. Una explicación cualitativa del la observación se da en términos de una ecuación tipo Burger para la curvatura.

Descriptores: Cápsula; ondas; flujo de Poiseuille.

PACS: 46.40.-f; 83.50.-v

1. Introduction

The study of the behavior of capsules in Poiseuille flow has received a great deal of attention due to the relevance to studies of the behavior of red cells in blood vessels. The continuum models for the membrane stresses, including effects of bending, have been proposed and studied for capsules in simple shear flow in the fundamental studies of Pozrikidis [1].

Subsequent simulations have been used to study the behavior of capsules in Poiseuille flow. In particular to better understand the lateral migration of capsules in Poiseuille flow, Doddi and Bagchi have presented a complete study [2] with relevant references provided in this work. Recently, the study of the change of shape of capsules has been undertaken using, on one hand, particle dynamics –to describe the flow field– and, on the other, a discrete description of the membrane in terms of the energy of stretching and bending energies [3]. In these studies, a transition from discoidal to V shaped capsules is documented. This depends on the flow velocity and the bending rigidity of the membrane.

The present two-dimensional study is complementary in several ways to the one mentioned above. In the first place, using a continuum description of the membrane form, its deformation was studied in Poiseuille flow. For drops as well as capsules, we find, as in [2], that two vortices form inside the vesicles. For drops a high curvature static region on its trailing edge is observed, with larger curvatures for higher flow velocities. When bending effects are taken into account, the high curvature region generates a traveling wave along the membrane. This wave, as it travels along, separates the regions of positive and negative curvature, leading ultimately to the transition from discoidal configuration to the V-shape observed experimentally and numerically in Ref. 3 to 5 for capsules.

In this work it is shown numerically that the traveling wave propagates with constant velocity along the capsule's membrane. The dependence of the velocity on the applied pressure gradient and the extensibility of the capsule is studied. We can thus provide a qualitative explanation of the resulting terms of a Burger's type equation.

This Note is organized as follows. In the second section we formulate the problem and describe the numerical solution. The third section is devoted to a description of the results whereas the last section provides the Conclusions.

2. Formulation of the problem and numerical solutions

The problem of the two-dimensional motion of a drop or capsule in a prescribed Poiseuille flow geometry –as shown in Fig. 1– is presented, for the velocity $\mathbf{u}_1$ and pressure p_1 fields of the ambient —external— flow, and $\mathbf{u}_2$ and pressure p_2 fields for the inner flow respectively. The flow is assumed to be Stokes flow. The capsule is described by the moving curve $C(t)$, parametrized by $\mathbf{x}(s,t)$ with normal $\mathbf{n}$. This surface region, enclosing region Ω_2 and shown in Fig. 1, satisfies the kinematic conditions

$$\frac{d\mathbf{x}(s,t)}{dt} = \mathbf{u}_1\left(\mathbf{x}\left(s,t\right)\right) = \mathbf{u}_2\left(\mathbf{x}\left(s,t\right)\right) \qquad (1)$$

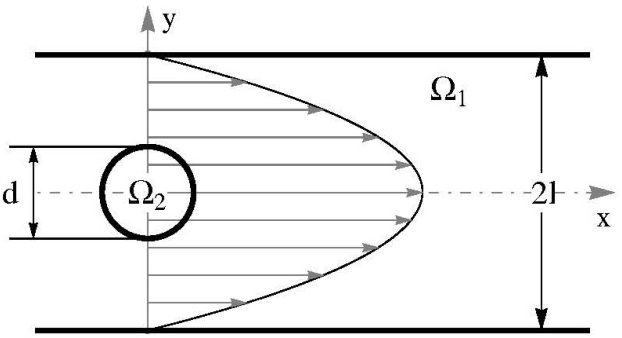

FIGURE 1. Basic geometry.

The fluid inside the capsule —within Ω_2— satisfies the Stokes equation:

$$\nu_2 \Delta \mathbf{u}_2 = \nabla p_2,$$
$$\nabla \cdot \mathbf{u}_2 = 0. \tag{2}$$

The ambient fluid satisfies Stokes flow equation in Ω_1 for the region outside the drop and between the parallel walls at $y = \pm l$ namely:

$$\nu_1 \Delta \mathbf{u}_1 = \nabla p_1,$$
$$\nabla \cdot \mathbf{u}_1 = 0. \tag{3}$$

with $\mathbf{u}_1 = \mathbf{0}$ on $y = \pm l$. Given that our interest is in the motion of the drop or capsule in an imposed Poiseuille flow, with velocity profile as shown in Fig. 1, then the boundary condition is

$$\mathbf{u}_1 \simeq \left(\frac{p_x}{2\mu} \left(y^2 - l^2 \right), 0 \right) \qquad \text{as} \quad |\mathbf{x}| \to \infty, \tag{4}$$

where p_x is the negative constant pressure gradient along the flow to be satisfied. Boundary conditions at the interface are specified by continuity of the velocity field —kinematic condition— Eq. 1, and a prescribed jump in the normal stresses which depend on the model for the mechanical properties of the interface.

The tension of the membrane or capsule, which is parametrized by the arc-length s, is given by

$$\mathbf{T} = \gamma \tau + q\mathbf{n}, \tag{5}$$

where τ and $\mathbf{n}$ are the unit tangent and unit normal to $C(t)$, respectively. The function γ is the elastic tension. The function q that accounts for the bending, with $q = dm/ds$, where the bending moment, in the form $m(s) = \rho\, K(s)$, is related to the local curvature of the vesicle $K(s)$.

The stress balance on the interface $C(t)$ gives for the jump $\Delta \mathbf{f}$ of the normal component of the fluid stress tensor in the form:

$$\Delta \mathbf{f} = -\frac{d\mathbf{T}}{ds} = \left(\gamma\, K(s) - \rho \frac{d^2 K}{ds^2} \right) \mathbf{n}$$
$$- \left(\rho\, K \frac{d\, K}{ds} + \frac{d\, \gamma}{ds} \right) \tau. \tag{6}$$

The latter equation closes the system for the evolution of the interface. In the case of inextensible capsules, γ is taken as a constant and corresponds to the surface tension, and ρ is taken to be zero because its rigidity is neglected. For capsules, the bending moment contribution has a normal direction component K_{ss}, which regularizes the term $\gamma\, K$ when large gradients of K are present. This term will be shown to be responsible for the traveling of the inflection point of the curvature along the membrane.

In biological membranes [1], it is known that γ may depend on the state of compression or extension of the membrane; this rate is given by considering $\lambda_s = \partial\, S\,(s_0, t)\,/\partial s_0$, which is the rate of extension relative to the initial reference configuration parametrized by s_0.

Taking $\gamma = E(\lambda_s - 1)$ gives an interfacial tension contribution when the membrane is stretched, and a negative contribution for compressed interfaces. At each point, and in order to calculate the corresponding deformations, it is necessary to know $s_0 = s_0\,(s, t)$ as a function of the position along the current interface.

The equations to be solved are the fluid equations—(2) and (3)—, coupled with the kinematic condition, (1), and the dynamic equation, (6), respectively.

These equations are solved numerically using the boundary integral formulation [8] reducing the problem to the solution of an integral equation on the boundary $C(t)$, which gives the velocities of the external fluid —$\mathbf{u}_1\,(\mathbf{x} \in C(t))$— in terms of the imposed flow, and the jump in stress, which is given by (5) in terms of the shape of $C(t)$.

3. Numerical solution

In this formulation we denote by $\mathbf{G}$ the Green's Function for the channel with zero boundary conditions on the walls. In this case, for the $\mathbf{G}$ matrix we have:

$$\mathbf{G}\,(\mathbf{x}, \mathbf{x}_0) = -\ln |\mathbf{x} - \mathbf{x}_0|\, \mathbf{1}$$
$$+ \frac{(\mathbf{x} - \mathbf{x}_0)\,(\mathbf{x} - \mathbf{x}_0)}{|\mathbf{x} - \mathbf{x}_0|^2} + \mathbf{G}_w\,(\mathbf{x}, \mathbf{x}_0)\,. \tag{7}$$

Here, $\mathbf{G}_w\,(\mathbf{x}, \mathbf{x}_0)$ is the sum of images needed to satisfy the boundary condition of zero velocity at the walls. The third-order traction tensor is also expressed in the form:

$$\mathbf{T}\,(\mathbf{x}, \mathbf{x}_0) = -4 \frac{(\mathbf{x} - \mathbf{x}_0)\,(\mathbf{x} - \mathbf{x}_0)\,(\mathbf{x} - \mathbf{x}_0)}{|\mathbf{x} - \mathbf{x}_0|^4}$$
$$+ \mathbf{T}_w\,(\mathbf{x}, \mathbf{x}_0)\,. \tag{8}$$

where $(\mathbf{x} = \mathbf{x} - \mathbf{x}_0)$ Following the usual procedure [8-10] of multiplying (2) and (3) by the Green's function $\mathbf{G}$ and integrating by parts to transform the integrals into boundary integrals, which are subsequently evaluated using the boundary

conditions, we obtain the integral equation for the velocity $\mathbf{u}_1$ on the boundary of the vesicle in the form:

$$\frac{1+\lambda_\mu}{2}\mathbf{u}_1(\mathbf{x}) - \frac{1-\lambda_\mu}{4\pi}\int_C \mathbf{u}_1(\xi)\cdot\mathbf{T}(\mathbf{x},\xi)\cdot\mathbf{n}(\xi)\; dl(\xi)$$

$$= \mathbf{u}_\infty(\mathbf{x}) - \frac{1}{4\pi\mu_1}\int_C \mathbf{\Delta f}(\xi)\cdot\mathbf{G}(\mathbf{x},\xi)\; dl(\xi) \qquad (9)$$

where λ_μ is the ratio of viscosities for $\mathbf{x}\in C(t)$. When the vesicle is small compared with the size of the channel, then $d/l \ll 1$, and the image contributions to the motion of the drop are small; *i.e.*, $\mathbf{G}_w(\mathbf{x},\mathbf{x}_0)$ and $\mathbf{T}_w(\mathbf{x},\mathbf{x}_0)$ being smaller than the leading term. The integral equation is solved rapidly using this approximation.

Then given the initial curve, $\Delta\mathbf{f}$ is computed using (6). The integral equation is solved and the velocity field $\mathbf{u}_1(\mathbf{x})$ is obtained. This velocity is then used in the equation

$$\frac{d\mathbf{x}}{dt} = (\mathbf{u}_1\cdot\mathbf{n})\mathbf{n} \qquad (10)$$

to advance the surface, and the process is repeated. The discretization of the integrals with arc segments as proposed by [8] is used. The consistency of the method was checked by doubling the number of segments with no appreciable changes in the solution. The simulations show that the evolution of the drop continues for long times without numerical instabilities.

4. Results

We begin by considering the evolution of a drop with sizes $d = 1$ inside a channel of size $l = 4$. The nondimensional pressure gradient of the Poiseuille flow is $p_x = 1$, the interfacial tension $\gamma = 1$, and this gives a capillary number $Ca = 0.5$.

In Figs. 2a – 2c the time evolution of the drop is shown for $t = 0$, $t = 2$, $t = 3.5$. Inside the drop, two vortices are present. It is clear that the drop inverts the curvature at the trailing edge.

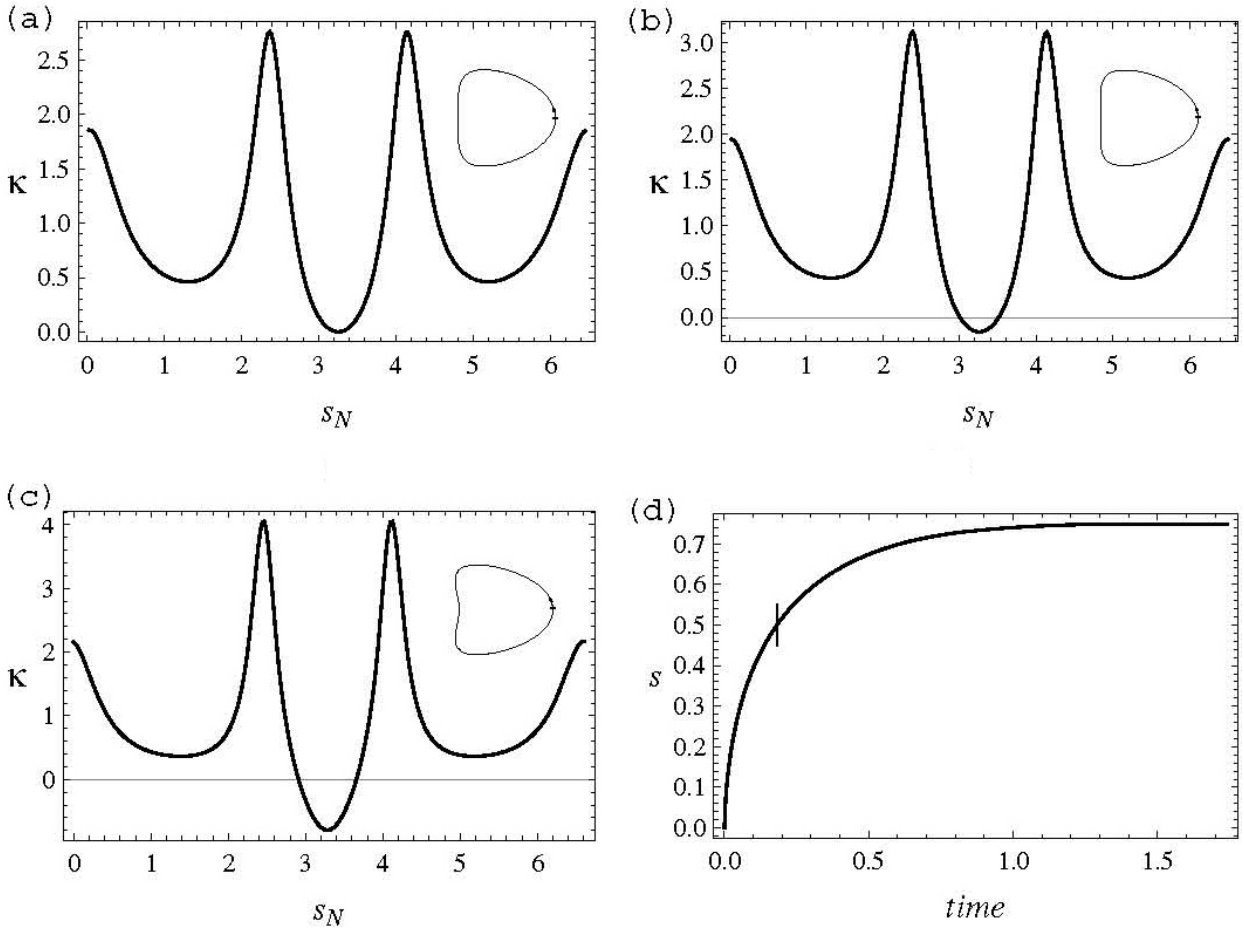

FIGURE 2. The time evolution of the drop with a flow of $Ca = 0.5$. The curvature plots for (a) $t = 0$, (b) $t = 0.1875$, and (c) $t = 1.7425$ –after the first arc segment reaches a curvature of zero– show a small invasion of the region of negative curvature when the steady state in (c) is obtained. (d) shows the rapid transient leading to the steady state with small deformation.

The curvature is plotted as a function of the arc-length parameter. We observe in the trailing edge a region in the center where the curvature changes sign. This region then expands. The zero curvature value indicates the position of the position of the curvature front along the back end of the drop. In Fig. 2c the position of the front is shown as a function of time. It also shows that the negative curvature region grows and rapidly settles (at least numerically) to an asymptotic state.

We can give a qualitative explanation of this evolution by obtaining a simplified equation for the evolution of the curvature as follows. To obtain $\mathbf{u}_1$, the first iterate is used as an approximation to the solution of the integral equation such that

$$\mathbf{u}_1\left(\mathbf{x}\left(s,t\right)\right) \doteq \mathbf{u}_\infty\left(\mathbf{x}\left(s,t\right)\right) - \frac{1}{4\,\pi\mu_1}\int\limits_C \mathbf{\Delta f}\cdot\mathbf{G}\,\left(\mathbf{x},\xi\right)\,dl\left(\xi\right). \qquad (11)$$

The integral is approximated with the mean value to obtain

$$\mathbf{u}_1\left(\mathbf{x}\left(s,t\right)\right) \doteq \mathbf{u}_\infty\left(\mathbf{x}\left(s,t\right)\right) - \frac{1}{4\,\pi\mu_1}\mathbf{\Delta f}\left(\mathbf{x}(t)\right)\int\limits_{C(t)} \mathbf{G}\,\left(\mathbf{x},\xi\right)\,dl\left(\xi\right). \qquad (12)$$

For the case of a drop, *i.e.*, $\Delta\mathbf{f}(\mathbf{x}(s,t)) = K\,\mathbf{n}$, the approximate equation for the evolution of the boundary is:

$$\frac{d\,\mathbf{x}\left(s,t\right)}{dt} = \mathbf{u}_\infty\left(\mathbf{x}\left(s,t\right)\right) + h\left(t\right)\,K\left(s,t\right)\,\mathbf{n}\left(s,t\right), \qquad (13)$$

where

$$h\left(t\right) = \int_C \mathbf{G}\,\left(\mathbf{x},\xi\right)\,dl\left(\xi\right).$$

Now, from (13) an equation for the curvature can be obtained. To this end, recall that $K(s,t) = \left(\dot{\tau}\cdot\dot{\tau}\right)^{1/2}$, where τ is the unit tangent vector $\tau = \mathbf{x}_s$, where s is the arc-length.

Using $\tau_s = K\,\mathbf{n}$, the evolution of the curvature is

$$\frac{d\,K}{dt} = \frac{1}{K}\mathbf{x}_{ss}\cdot\mathbf{x}_{sst} = \mathbf{n}\cdot\mathbf{x}_{sst}. \qquad (14)$$

The evolution of $\mathbf{x}_{ss}$ is obtained by differentiation of Eq. (13). After using $\dot{\mathbf{n}} = -K\,\tau_s$ in (14), the evolution for the curvature is given by:

$$\frac{d\,K}{dt} = \mathbf{n}\cdot\mathbf{u}_\infty\left(\mathbf{x}\right)_{ss} + h\left(t\right)\,\mathbf{n}\cdot\left(K_{ss}\mathbf{n} - K^3\mathbf{n} - KK_s\tau\right) \qquad (15)$$

Notice that (15) coupled with $\dot{\tau} = K\,\mathbf{n}$ and $\dot{\mathbf{n}} = -K\,\tau$ gives a closed set of equations since the term $\mathbf{u}_\infty\left(\mathbf{x}\right)_{ss}$ as a nonlocal function of τ and $\mathbf{n}$. Notice that the hyperbolic term $KK_s\tau$ is absent because $\mathbf{n}\cdot\tau = 0$. Then, if solutions with large gradients are considered, the dominant term in (15) is just the diffusion equation. Thus, it shows that changes in curvature do not propagate along the membrane. Thus, in this regime the balance is localized. As time evolves a cusp develops towards the interior of the drop, in a process similar to the one described in Ref 7, the latter being generated at the

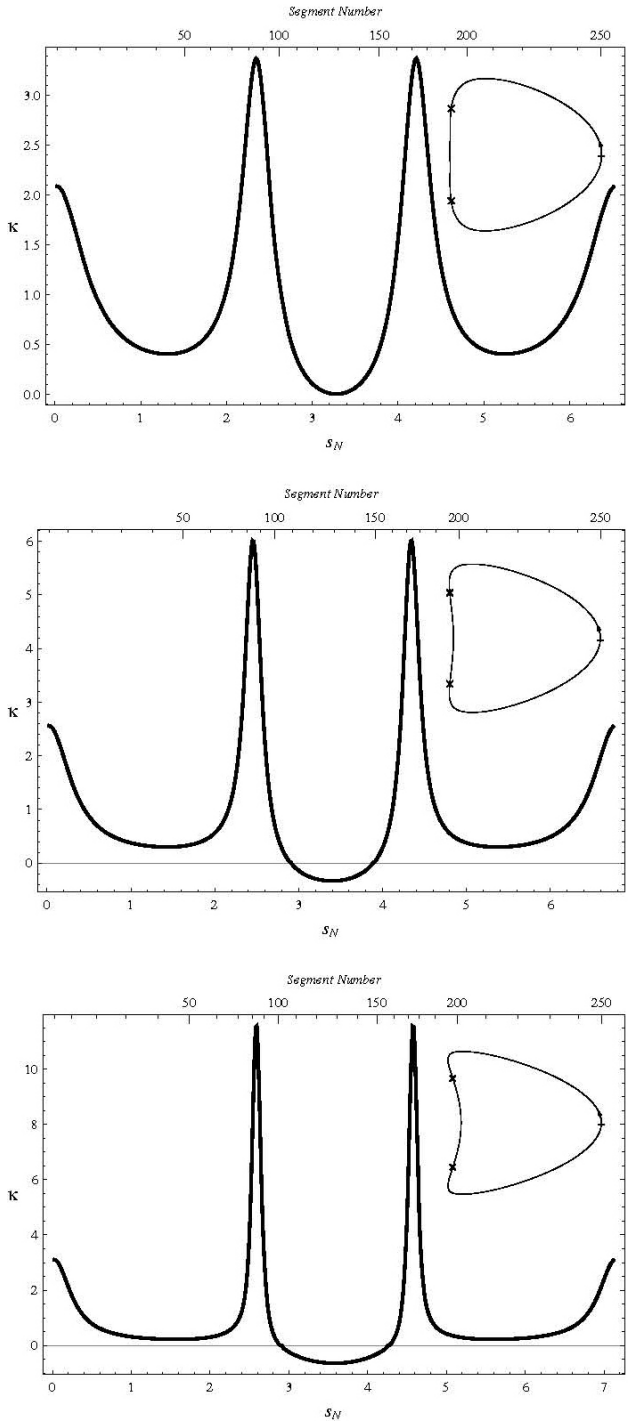

FIGURE 3. The time evolution of a capsule with $E = 0.5$, $\rho = 1$, and a flow of $Ca = 0.5$. The inserts show the form of the capsule whereas the curvature plots show the invasion of the region of negative curvature into the membrane deforming the capsule. Capsule forms after onset of negative curvature at (a) $t = 0$, (b) $t = 0.1675$, and (c) $t = 0.335$.

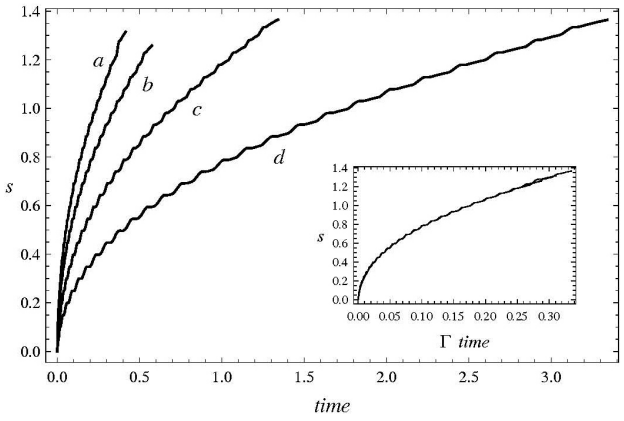

FIGURE 4. Plots of the wave front position as a function of time for $Ca = 0.5$, $\rho = 1$, and different extensibility by changing the pressure gradient of the flow. Here $\Gamma = p_x/2\mu$, and curve (a) $\Gamma = 0.1$, $E = 0.2$; (b) $\Gamma = 0.25$, $E = 0.5$; (c) $\Gamma = 0.5$, $E = 1.0$; and (d) $\Gamma = 0.75$, $E = 1.5$. The insert shows that the evolution arc is self-similar provided that the time is scaled within the corresponding shear rate.

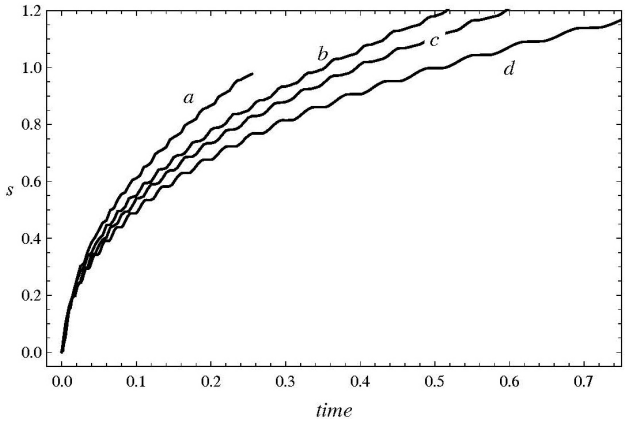

FIGURE 5. Evolution of the front for different values of the capsule rigidity and different capillary number of the flow. The parameters are: $\rho = 1$, and the values for (a) $Ca = 0.25$, $E = 2.0$; (b) $Ca = 0.5$, $E = 1.0$; (c) $Ca = 0.75$, $E = 0.667$; and (d) $Ca = 5.0$, $E = 0.1$.

free interface of fluid-air by a slightly immersed vortex dipole in the highly viscous liquid. The inner flow of the capsule is also generated by a vortex dipole.

Now, the effects of the extensibility of the membrane are considered. To this end, Fig. 3 displays the evolution of a capsule with bending moment $\rho = 1$, extensibility parameter $E = 0.5$ and $Ca = 0.5$. A relatively rapid propagation of the region of negative curvature can be observed, which is generated —as in the case of drops— by the inner vortices in the upper and lower portion of the capsule. This invasion front disturbs substantially the capsule due to the finite extensibility.

This curvature front (which is absent in drops) travels with an almost constant speed along the membrane. This markedly different behavior is due to both the membrane extensibility and the presence of the bending moment, which acts as a regularization for the evolution of the curvature while preventing the formation of sharply turning interfaces. Also, for the extensible capsule the curvature of the traveling wave does not increase after the capsule, has been bent.

Figure 4 details the evolution of the fronts for different pressure gradients with a constant capillary number as shown in the figure. Larger pressure gradients produce faster motion of the fronts. It can be also observed that the motion is self-similar with the same asymptotic shape provided that time is scaled with the corresponding shear rate.

Finally, we studied the behavior of the front as a function of the rigidity E for constant values of the flow. It can be observed that the front travels faster with larger values of the rigidity. These results are displayed in Fig. 5.

These effects can be explained qualitatively as before considering in the derivation of (14) those effects due to the extensibility and the bending moments. The same argument used for the drop is readily modified using an appropriate $\Delta\mathbf{f}(\mathbf{x}(t))$ for the capsule. In this case, the most nonsingular terms give:

$$\frac{d\,\mathbf{x}\,(s,t)}{dt} = h\,(t)\;\{\lambda\,(s,t)\,K + \rho\,K_{ss}\}\,\mathbf{n}\,(s,t)\,, \qquad (16)$$

where now the local extension $\lambda(s,t)$ is no longer constant. Again, the same procedure gives a diffusion equation with a hyperbolic term, which comes from λ_s. Thus,

$$\frac{dK(s,t)}{dt} = h(t)\,\{E\lambda_{ss}\,(s,t)\,KK_s - \lambda K_{ss} - \rho K_{ssss}\}\,. \quad (17)$$

This equation —that to leading order is Burges Equation with variable coefficients— sustains traveling fronts that are regularized shocks of the nonlinear hyperbolic equation. The solution of the equation demonstrate that as the rigidity E increases $E\,\lambda_{ss}$ also grows, giving a larger speed of propagation of the front as shown in Fig. 5. The results of Fig. 4 can be explained as follows: as the flow increases, the inner cortices become stronger and the curvature perturbation is larger as well. The perturbation of the membrane decouples from the flow and evolves according to Burges' equation. In this case, larger perturbations travel faster and this explains the results of Fig. 4. It is to be noted that the wiggly behavior of the curves is an effect of the discretization and the fact that a term of fourth-order derivatives of the curvature needs to be resolved.

5. Conclusions

In this study we found that capsules do sustain traveling waves of bending along their membrane while subjected to Poiseuille flow. The waves originate from the curvature gradient of the trailing edge of the vesicle, which is balanced by the extensibility of the membrane and the bending moment, producing a wave of diffusion of curvature. We also obtained that the velocity of the curvature wave increases with the pressure gradient, and with the rigidity. This type of behavior

was qualitatively explained in terms of a drastic approximation leading to a nonlinear advection–diffusion equation for the curvature, which accounts for all the observed features. However, to obtain the precise information, the detailed numerical study is required.

Acknowledgments

We thank PROFIP-DGAPA of UNAM for their continued support and encouragement, as well as CONACyT for funding of this research work.

1. C. Pozrikidis, *The IMA Volumes in Mathematics and Its Applications* **221** (2001) 189.
2. S.K. Doddi and P. Bagchi, *International J. of Multiphase Flow* **34** (2008) 966.
3. Tsorng-Whay Pan and T. Wang, *International J. of Numerical Analysis and Modeling* **6** (2009) 455.
4. H. Noguchi and G. Gompper, *Proc. National Academy of Sciences* **102** (2005) 14159.
5. V. Vitkova, M. Mader, and T. Podgorski, *Europhys. Lett.* **68** (2004) 398.
6. J.J. Herrera, A.A. Minzoni, and R. Ondarza, *Physica D* **57** (1992) 249.
7. Y.D. Shikhmurzaev, *Capillary flows with forming interfaces* (Chapman & Hall/CRC 2008).
8. C. Pozrikidis, *Boundary Integral and Singular Methods for Linearized Viscous Flow* (Cambridge Univ. Press, USA. 1992).
9. C. Pozrikidis, *A Practical Guide to Boundary Element Methods with the Software Library BEMLIB* (Chapman-Hall/CRC Press, USA. 2002).
10. L. Gary Leal, *Advanced Transport Phenomena*. (Cambridge Univ. Press, USA. 2007).